Characterization of a Bouc-Wen model-based damper model for automobile comfort simulation

Hanwei GAO[1,2], Louis JÉZÉQUEL[1], Eric CABROL[2], Bernard VITRY[2]

[1]LTDS, Ecole Centrale de Lyon, UMR5513, 69134, Ecully Cedex, France
hanwei.gao@ec-lyon.fr
[2]Technocentre Renault, 78280, Guyancourt, France

Abstract

Ride comfort is considered as one focus for a chassis system. To ensure a satisfying comfort performance of a vehicle in development, a detailed damper characterization needs to be pre-defined in the early phase of project with the help of simulation results in virtual proving ground. However, the current damper model integrated in whole vehicle simulations is sometimes difficult to fit to test results due to its over-simplifications especially in low speed excitation regimes. Thus this article proposes an enhanced shock absorber model to improve simulation predictions without increasing substantially calculation costs. The parameterized model is mainly based on a modified Bouc-Wen model considering its capability of reproducing highly nonlinear hysteretic phenomena. In order to identify the parameters, a multi-objective optimization using NSGA-II algorithm has been applied. The excitations on test bench have been separated into several groups according to their force-velocity curve shapes. Finally an optimum set which represents the compromises between the objectives is obtained and forms a Pareto front. Comparative examples in virtual proving ground show that the correction quality is well improved for chassis' comfort prediction using the proposed model. This example demonstrates the effectiveness of the modelling and its potential in comfort improvement with the help of design of experiments.

1 Introduction

Ride comfort is one of the focuses of vehicle suspension design. To ensure that the comfort performance has been satisfied, the technical specification has been defined at the early stage of new vehicle projects and then validated after the chassis system is designed. With the development of numerical technologies, the prediction of ride comfort at an earlier phase of project is becoming important because several specifications need to converge at the same time and the unsatisfied comfort specification may cause the retreat of the designing choices during validation stage.

One main difference between simulations for ride comfort and simulations for other specifications such as chassis durability or dynamic behaviour is that the low velocity regime of the shock absorbers is more important since it plays a critical role to filter small road oscillations [1] . In order to improve the quality of prediction by comfort simulations, a detailed damper model which is capable of reproducing the physical damping forces around zero velocity is searched. In virtual proving ground simulation, several damper models are proposed.

The classical way is to define a one-to-one look-up table between force and velocity according to the measurements. A single curve with several slopes is easy to define at the early development stage and this model requires the least calculation resources. So it is commonly used in durability test track simulations, where the acceleration peaks with high velocity will cause more damage to chassis components. However, the single curve model may be over-simplified in low velocity regime where hysteresis force tends to 'open' the damping curve. As a result, more details should be extracted from the measurements and included in the model.

The second way is to construct a semi-physical damper model through a combination of several sub-models such as spring, damper or friction parts. These parts can be expressed in analytical expressions by partial-derivative equations, which cost larger but still acceptable calculation resources. The main difficulty of application is to find the parameters of these sub-models which cannot be derived directly from physical construction of components. Different identification methods have been developed based on the experimental data ([2–5]) . In [4], it has been shown that this model is suitable for real-time hardware-in-the-loop simulations.

The third way is to construct a physical damper model which aims at simulating the phenomena in real components, such as the circulation of oil. The physical parameters such as the piston diameter and valves' opening pressures need to be identified basing on real shock absorbers. However, the influence of these parameters on damping curves may be indirect and thus it is hard to be predefined in early development phases. This kind of model is usually provided by shock absorber suppliers as a black-box model. In [6, 7], a model established in AMESim has been proposed and it can be integrated into virtual proving ground by co-simulation. It is theoretically the most precise but takes the longest time to solve.

An alternative way is to identify a data-driven model without concerning its physical characters [8]. The method is efficient when the physical modelling is too complex to be identified or some specific characters may be neglected because of its complexity. However, as in virtual ground simulation, it is preferable to keep some physical relations into shock absorbers as a reference for further designing.

In this paper, the semi-physical method is selected as it is the compromise between the single-curve model and the physical model in terms of configuration process and calculation costs. Another advantage of the functional model is that it is easy to reconstruct each sub-model in MSC ADAMS/Car environment without introducing a third software for co-simulation, which makes it more user-friendly to deploy the method in vehicle projects. Before being integrated into a full-vehicle simulation, the damper model is first identified by a multi-objective optimization algorithm, which is also used in [9, 10] for a Bouc-Wen model. However, based on the measurements it is shown that a set of parameters is not capable of satisfying all the excitations with different frequencies or velocities for a given shock absorber. By contrast, by separating the objectives into several groups, a set of non-dominated optimums can be obtained and then the model parameters can be decided according to the type of frequency needed.

Part 2 of this paper summarizes the friction models, especially Bouc-Wen one. Part 3 introduces the Bouc-Wen based damper model and its identification process using a multi-objective optimization plan. Part 4 applies the proposed model into a full vehicle comfort simulation, which indicates that the new model can produce better test correlation than a single damper curve.

2 Hysteresis models

A vehicle suspension shock absorber is based on a mono-tube or bi-tube technology. One of the difficulties is its non-linear hysteresis response which is non-negligible in low velocity regime. Different models have been proposed to model the hysteresis phenomenon which is a combination of the effect of oil viscosity and interior friction. In Renault, the measurement procedure of a shock absorber is realized by a series of sinus excitations with different amplitudes and frequencies. Figures in Table 1 have shown the strong non-linearity character of a measured shock absorber. The force-velocity curve may be very different with the same damping velocity but different excitation frequencies. To model this phenomenon, several sub-models are introduced.

2.1 Coulomb friction model

This is the basic friction model. The friction force changes direction with the velocity, but its absolute value is a constant. The mathematical equation can be expressed as

$$f = -sign(v)F_{Coulomb} \tag{1}$$

where the signum function $sign(x) = \begin{cases} 1 & x > 1 \\ -1 & x < -1 \end{cases}$, v is the damping velocity, $F_{Coulomb}$ is the constant friction force. However, the discontinuity at the zero velocity may cause numeric problems in simulation [4].

2.2 Dahl model

The Dahl friction model can solve the discontinuous problem of Coulomb model by introducing two more variables σ_0 and i. It was first proposed by P.R Dahl in 1969 [11]. The equations of the model are

$$\begin{gathered} f = \sigma_0 u \\ \dot{u} = v \cdot sign(1 - sign(v)\frac{\sigma_0 u}{F_c})|1 - sign(v)\frac{\sigma_0 u}{F_c}|^i \end{gathered} \tag{2}$$

where u is a state variable, F_c is the maximum friction force which equals to the constant of Coulomb model [12]. σ_0 defines the stiffness of model and it can be translated to the slope of the curve when $F = 0$. When $\sigma_0 \to \infty$ the model will approach the Coulomb model. i models the shape of the curve at the beginning of the velocity change. The normalized friction force under different σ_0 and i are showed in Figure 1.

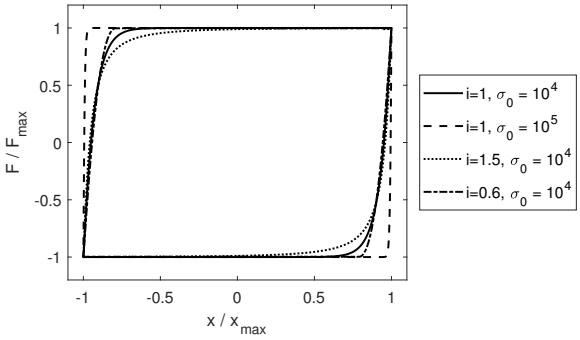

Figure 1 – Comparison of different parameters settings of i and σ_0 of Dahl model

2.3 Bouc-Wen model

The Bouc-Wen model gives a smooth description of the process from the elastic deformation to sliding between the contact surfaces. It was proposed by Bouc in 1967 and then developed by Wen. The equations of Bouc-Wen model [13] are

$$\begin{aligned} F &= cv + kx + f - f_0 \\ f &= \alpha z \\ \dot{z} &= \delta v - \beta v|z|^n - \gamma z|v||z|^{n-1} \end{aligned} \tag{3}$$

where F is the total damping force and f is the hysteresis force. x is the relative displacement of two ends of the shock absorber and v is the damping velocity. c is the viscous coefficient. k is the stiffness of the damper and f_0 is preload. Each part of the total damping force is described in Figure 2. In the hysteresis sub-model αz, z is a state variable. α defines the maximum hysteresis force which is equivalent to F_c in Dahl model. δ defines the linear stiffness of the hysteresis part. β, γ define its non-linear stiffness and damping character. n has an influence on the smoothness of the system. Figure 3-5 show the influence of each parameters.

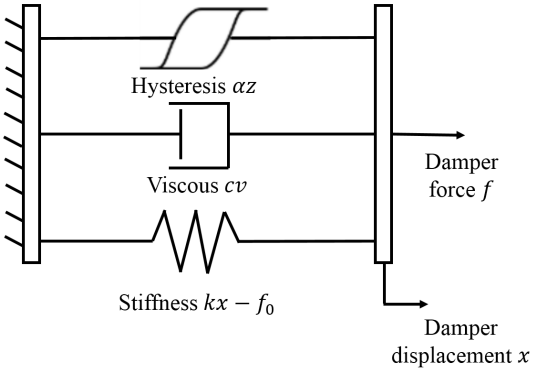

Figure 2 – Construction of the Original Bouc Wen model

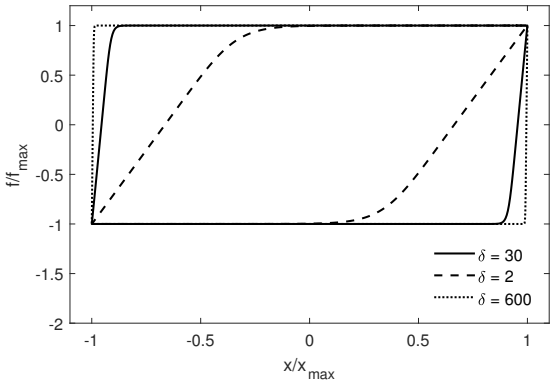

Figure 3 – Influence of δ on Damper force-displacement curve

Bouc-Wen model can reproduce different shapes under various excitation frequencies (see Figure 6). In contrast, there are more parameters to be identified than Dahl model:$c, k, \alpha, f_0, \delta, \beta, n$.

In addition, Ref [14] has extended the model to better correct non-symmetric hysteretic responses around zero velocity. It is called "shifted hysteresis".The hysteresis part of (3) can be rewritten as the function of v

$$\dot{z} = (\delta - (\beta + \gamma sign(zv))|z|^n)v \tag{4}$$

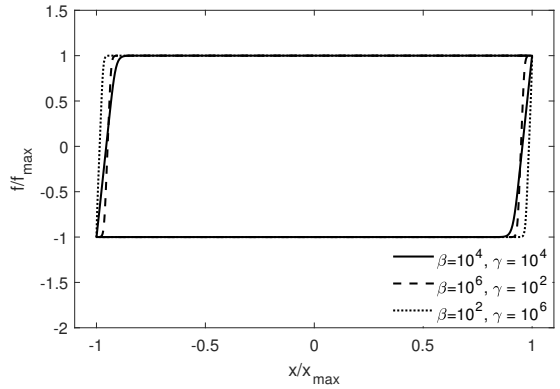

Figure 4 – Influence of β and γ on Damper force-displacement curve

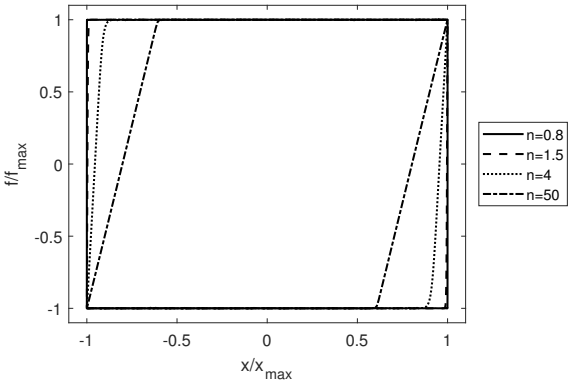

Figure 5 – Influence of n on Damper force-displacement curve

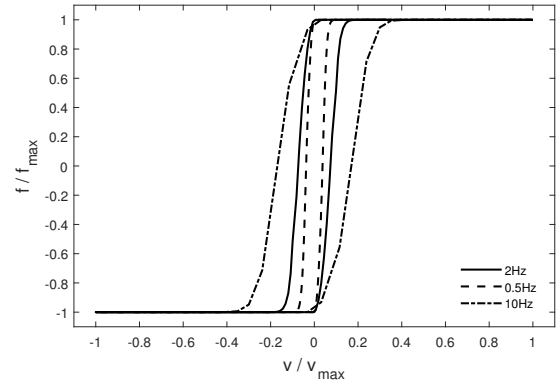

Figure 6 – Hysteresis curve under different excitation frequencies

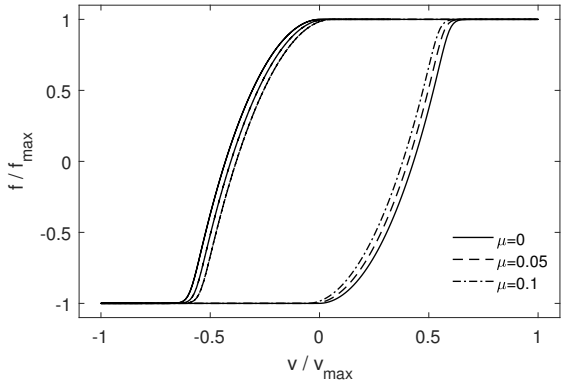

Figure 7 – Influence of μ on Damper force-displacement curve

then v is replaced by a shifted velocity which is defined as

$$v \leftarrow (v - \mu \cdot sign(v)) \tag{5}$$

where μ is one additional parameter to be identified. The main effect is to modify the hysteresis curve around zero velocity without changing that of higher velocity (see Figure 7).

3 Parameter identification process

3.1 Model description

In Equation (3) and Figure 2, the original Bouc-Wen model is composed of several sub-models: spring part $(kx + f_0)$, viscous part (cx) and hysteresis part (αz). In this article, a modified Bouc-Wen model where the spring part and viscous part have been redefined is proposed. It serves as a template of which the parameters are to be identified basing on measurements. The construction of the model is shown in Figure 8. The whole modified Bouc-Wen model has been firstly established in Simulink for identification before being integrated into the vehicle model in virtual proving ground simulation environment in MSC Adams/Car.

3.1.1 Viscous model

The viscous part normally takes the majority of total damper force, and it is defined as a function of damping velocity. In this model, the linear relation has been replaced by a continuous function created from a look-up table which groups the maximum damping velocity measured at compression and rebound phases with the maximum force. Figure 9 shows an example of a test curve, where a strong non-linearity is observed. The

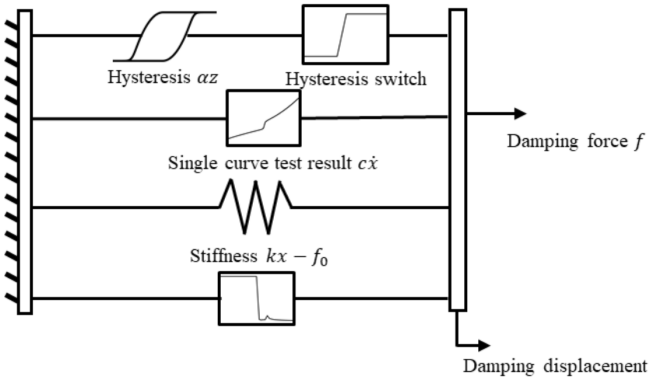

Figure 8 – Construction of a modified Bouc-Wen model

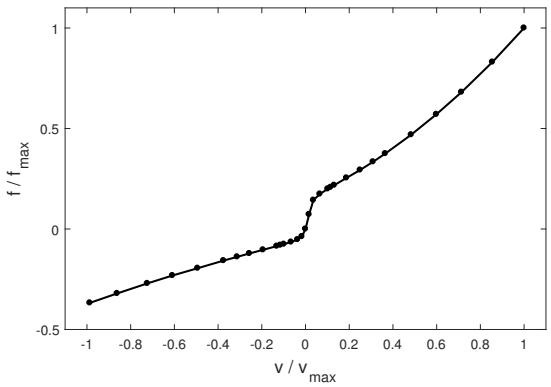

Figure 9 – Example of a single damping curve

viscous model serves as a basic line for the damper force which is previously used as the damper model in virtual proving ground simulation. By linear interpolation, the look-up table can translate the test data with an acceptable accuracy and good calculation efficiency. However, it considers only the peaks and troughs in the measured curves and thus the transformation information between the two is lost. The following sub-models aim to further exploit the test results.

3.1.2 Spring model

When the shock absorber is under excitation of very low velocity (for example, $< 0.01 m/s$), the force of gas compression becomes dominant compared to viscous force. The shock absorber behaves like a spring. The spring model is to model the gas compression character of a shock absorber where the force depends on the damping displacement. In the original Bouc-Wen model, this force is linear to the displacement with a slope of k and a preload f_0. Ref [4] states that sometimes the linear model fails to perfectly represent the gas force and the quadratic gas force model can solve this problem. The equation of the spring model thus can be expressed as

$$F_{gas} = Ax^2 + Bx + C \tag{6}$$

where A, B, C are the spring model parameters. In the test progress, C is the preload after installation. A and B can be found with quasi-static excitations. But in some practical cases, the quasi-static test is absent because the test bench is not capable of producing a very low velocity excitation. The gas force is then considered as linear $(A = 0)$ with a slope calculated by two measurements of displacements. In this example, A still holds to zero as it is neglectable for small damping displacements and B and C are considered with a certain tolerance, thus are also involved into the group of parameters to be identified.

3.1.3 Hysteresis model

The Hysteresis model is the identification focus of a Bouc Wen model. From the measurement curve in Table 1 and in other test results, hysteresis phenomenon is more significant in rebound phase than in compression phase. In compression phase, the curve keeps 'closed' when velocity is larger than $0.2 m/s$, which is difficult to be reproduced by an original Bouc-Wen hysteresis sub-model. An additional switch has been added after the hysteresis model which aims to forcedly 'switch off' the hysteresis for large compression velocities. The modified hysteresis curve is showed in Figure 10.

3.1.4 Compensation curve

The compensation part aims to cancel the double-counted contribution of hysteresis model to the maximum damping force because the saturation viscous part has already involved in the viscous model. The hysteresis model is first characterized individually under several sinus excitations in order to identify the maximum Bouc-Wen force under excitation velocities. Then compensation curve is defined by another look-up table.

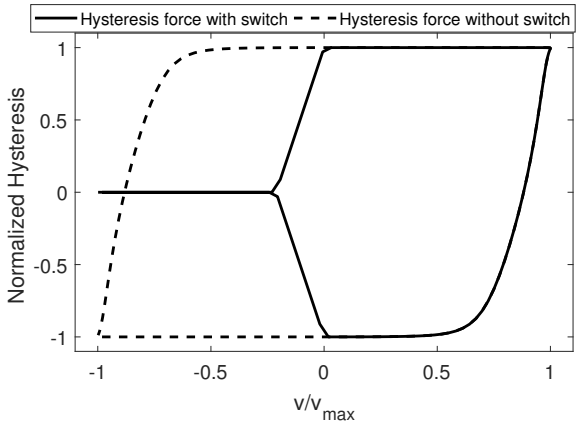

Figure 10 – The hysteresis force-velocity curve after passing the switch

3.2 Identification process

3.2.1 Optimization objectives

The model identification is to find the set of parameters which can produce the most similar damper character curves. The process can also be regarded as a multi-objective optimization plan aiming to minimize the quadratic errors between the model and the tests.

The algorithm schema of identification plan is showed in Figure 11. The same sinus signals are inputs to a physical shock absorber as well as the numeric model. The outputs of two models are differenced to obtain error signals, which are then post-treated to single indicators. The quadratic error of correction to i-th excitation (e_i) be defined as

$$e_i(\mathbf{x}) = \frac{1}{N}\sum_{j=1}^{N}(\varepsilon_i(\mathbf{x},t_j))^2 = \frac{1}{N}\sum_{j=1}^{N}(F_i(\mathbf{x},t_j) - \hat{F}_i(t_j))^2 \tag{7}$$

where $F(\mathbf{x},t)$ is the force sample at time t obtained from the numeric model with a vector of parameters $\mathbf{x}$. $\hat{F}_i(t_j)$ is the force curve from the test. $t_1, t_2..t_N$ are the sample points on $F(\mathbf{x},t)$ or $F_s(t)$. N is the total number of sample points. The optimization objective is to minimize $e(x)$. However, it should be noted that $e_i(x)$ contains not only the correction error but also disturbances such as the measurement noises on the test bench, so there is no meaning to pursue a model with zero correction errors which will result in an over-fitted problem.

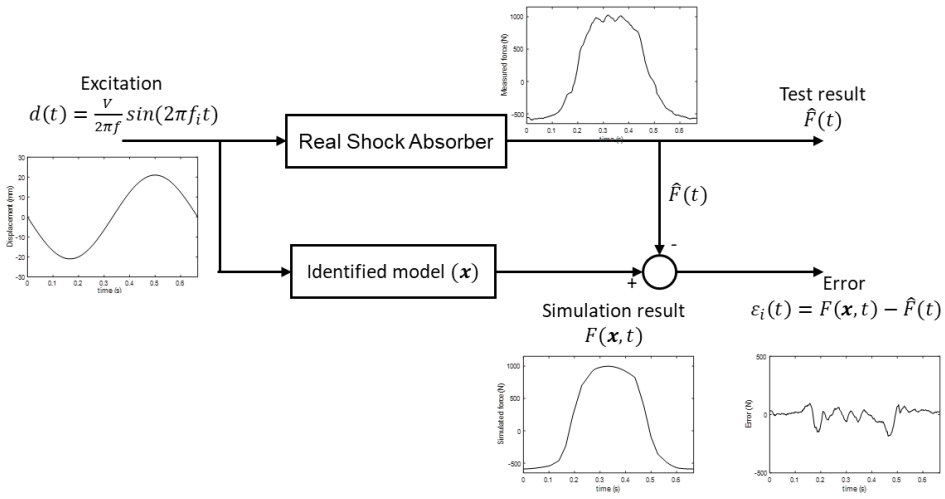

Figure 11 – The hysteresis force-velocity curve after passing the switch

A classical objective of identification is to minimize the sum of all the correction errors as shown in (8).

$$e_{total}(\mathbf{x}) = \sum_{i=1}^{M} e_i(\mathbf{x}) \tag{8}$$

where M is the total number of test excitations. The first attempt to find the best correction of the sum of all the excitations is not satisfying due to the damper's highly dissimilarity under different excitations in Table 1. The reason is that by summing all the errors the optimization has already a preference to a set of excitations. It is difficult to define a normalization factor of each objective at the beginning of the optimization which leads to satisfying results. Furthermore, the simple sum of all the objectives may result in an incomplete exploration of the designing space [9].

Group	LVLF	LVHF	HVHF
Velocity	0.1-0.4m/s	0.1-0.3m/s	0.5-1.2m/s
Frequency	1.5Hz	12Hz	12Hz
Nb. Signal	6	3	4
Curve example	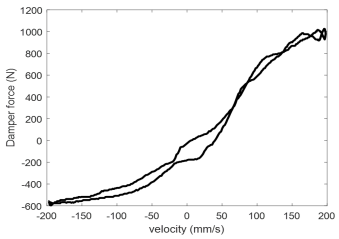	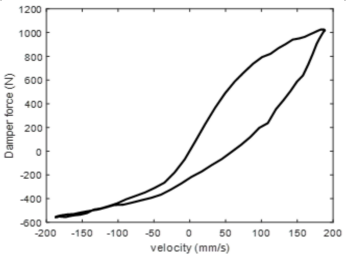	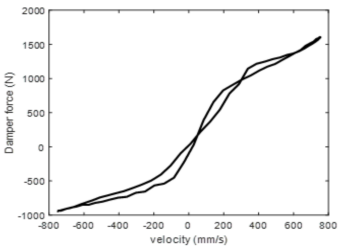

Table 1 – Repartion of Excitaion signals into several groups

Another approach is to separate the correction errors into several objectives when it is hard to find one dominating parameter set which minimizes all the errors. Thus, the test curves are attributed into several groups according to their curve similarities as well as the frequency regimes. Three groups have been defined for the shock absorber studied in Table 1: low velocity low frequency (LVLF), low velocity high frequency (LVHF) and high velocity high frequency (HVHF).

1. LVLF Group involves 6 excitations with maximum velocities smaller than 0.4m/s at the excitation frequency of 1.5Hz. In this group small hysteresis phenomenon is observed with a relatively closed curve and by the same time some irregular crossovers of the force may take place, which may be caused by the small measurement noise.

2. LVHF Group involves 3 excitations with maximum velocities smaller than 0.3m/s and excitation frequency is 12Hz. The shape of the test curve contains more hysteresis forces comparing to the same velocity excitations with 1.5 Hz. Here the highly dissymmetric hysteresis is also observed in the compression regime ($v < 0m/s$).

3. HVHF Group involves 4 excitations with maximum velocity between 0.5 and 1.2m/s at 12Hz. There is less hysteresis around zero velocity comparing to HVHF group and even less at higher velocities. So the shape of the curves is approaching a single curve model.

Then the objectives are defined as the average of the normalized mean quadratic errors in each of the groups. As the damper curves in each group are similar to each other so the sub-objectives are compatible.

$$\begin{aligned} e_{LVLF}(\mathbf{x}) &= \tfrac{1}{6}\textstyle\sum_{i=1}^{6} e_i(\mathbf{x})/e_i(\mathbf{x_0}) \\ e_{LVHF}(\mathbf{x}) &= \tfrac{1}{3}\textstyle\sum_{i=7}^{9} e_i(\mathbf{x})/e_i(\mathbf{x_0}) \\ e_{HVHF}(\mathbf{x}) &= \tfrac{1}{4}\textstyle\sum_{i=10}^{13} e_i(\mathbf{x})/e_i(\mathbf{x_0}) \end{aligned} \tag{9}$$

where $e_i(x)$ is the correction error defined in (7). It has been normalized by the correction results of the starting parameter sets x_0.

3.2.2 Optimization algorithm

To solve the multi-objective problem, a set of solutions which forms a Pareto front is to be searched. The Pareto front consists the non-dominated optimums where there exists no other solution that can improve one objective without degrading at least one another. A vector of parameters x^* can be defined as one Pareto optimum mathematically if and only if

$$\begin{aligned} &\forall x \in \varepsilon, \forall j \in \{1,...,m\}, f_i(x) < f_j(x^*) \\ &\Rightarrow \exists i \neq j, f_i(x) > f_j(x^*) \end{aligned} \tag{10}$$

With iterations the solution can converge to a potential Pareto front and all the points included in the front are optimized solutions. The Pareto front will collapse to one single point if it can minimize all the objectives and, in this case, the multi-objective optimization is equivalent to a mono-objective one.

The genetic optimization algorithm NSGA-II has been applied after the objectives and the design space are defined. NSGA-II can be viewed as a stochastic search method which explores the design space and selects the parent generation according to the fitness ranks of each existed solution to generate a new generation.

The optimization starts with an initial design of experiments to establish a relationship between the design space and the objectives by response surfaces. These response surfaces serve as the prediction functions from which a set of potential optimums is proposed before being validated by simulation. For the next iteration the former solutions will pass to a potentially better generations by selection, crossover and mutation operations [15]. The optimum sets proposed by the algorithm should finally be converged to a Pareto front. Figure 12 resumes the procedure of this optimization plan.

4 Identification results

4.1 Design space

In this chapter the identification model has been carried out on the shock absorber described in Table 1 as an example. All the designing parameters have been arranged in the vector **x**

$$\mathbf{x} = \{A, B, C, \alpha, \beta, \gamma, n, \mu\} \tag{11}$$

The initial, minimum and maximum values of these parameters are defined in Table 2. In this example, the gas pression forces are modelled linearly. Thus A remains to be zero.

	Initial value	Minimum Value	Maximum Value
A	0	0	0
B	-0.25	-0.5	-0.1
C	-150	-300	0
α	120	50	320
δ	30	10	600
$log(\beta)$	5.78	4	6
$log(\gamma)$	4.3	2	6
n	1.5	1.5	8
μ	0	0	0.001

Table 2 – Definition of design space

So the mathematical expression of the multi-objective optimization problem can be expressed as
Minimize:

$$F(x) = \{e_{LVLF}(x), e_{LVHF}(x), e_{HVHF}(x)\} \tag{12}$$

Under the constraints:

$$x \in DesignSpace \tag{13}$$

$F(x)$ is the target function used in generic optimization algorithm. Its compositions are the mean quadratic error of each group which defined in (9).

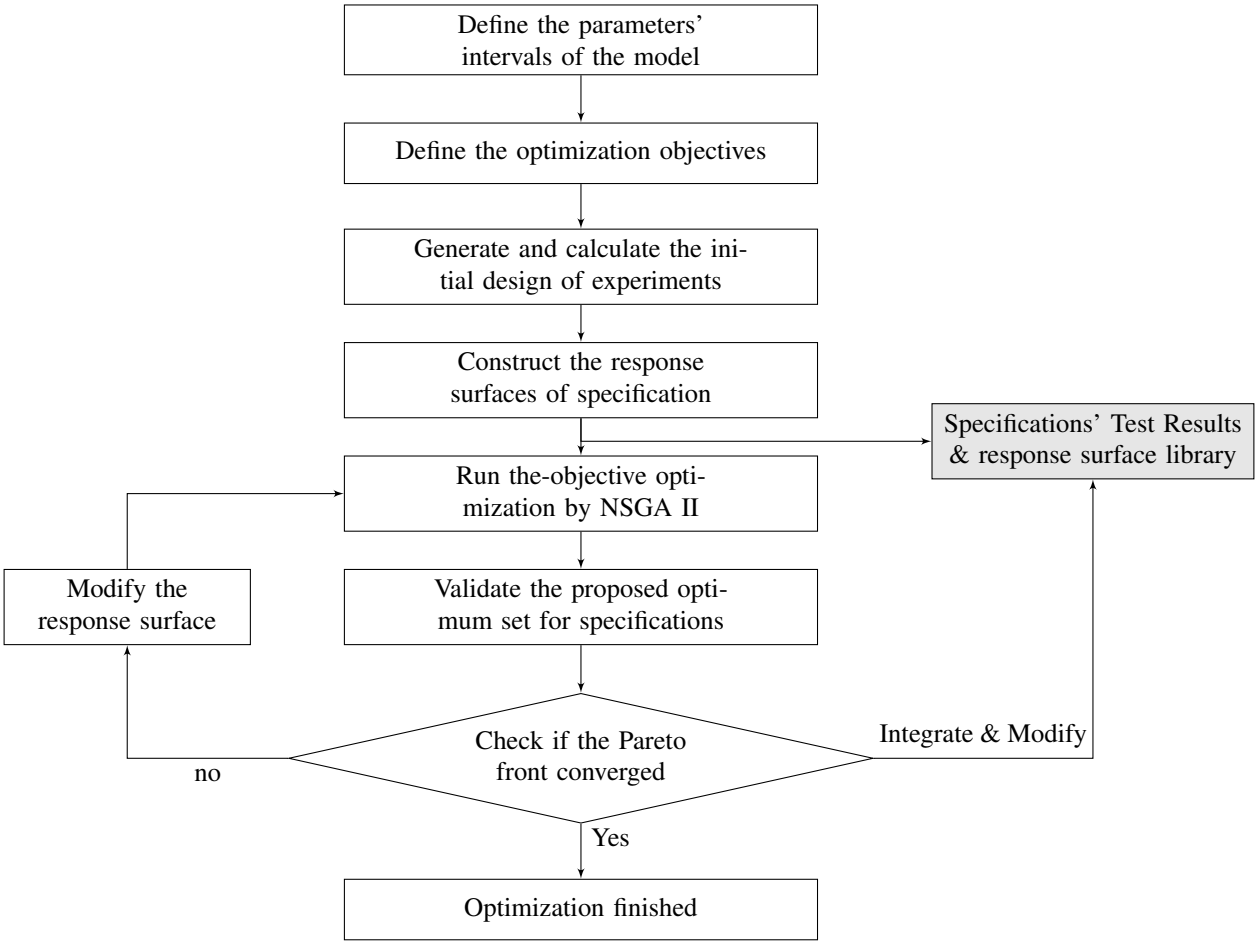

Figure 12 – Optimization process without robustness notions

4.2 Pareto fronts and surfaces

After 9 iterations, the correction objectives of non-dominated solutions are shown two-by-two in the Figure 13 and 14. The figure shows the correction objectives of three groups are incompatible especially between two different frequencies. Due to the complexity of the real shock absorber, the better correction to the low frequency signals may fit worse to high frequency ones and vice versa.

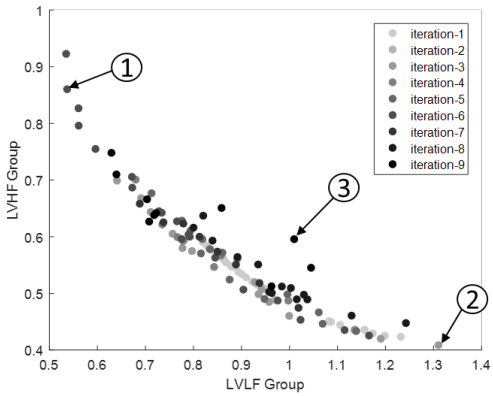

Figure 13 – Non-dominated solutions in LVLF-LVHF plane

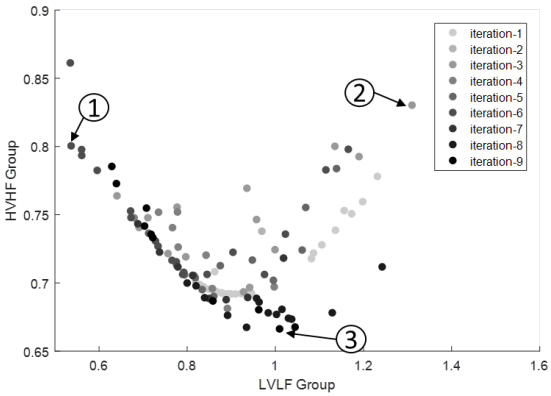

Figure 14 – Non-dominated solutions in LVLF-HVHF plane

Figure 15 shows the projection of the 3D Pareto surface on the LVHF-HVHF plan. The darker colour means better correction to LVLF group. This figure explains the reason why there are points far from the optimum front in Figure 13 and 14: The solution presented on one 2D Pareto front may not be involved in another 2D

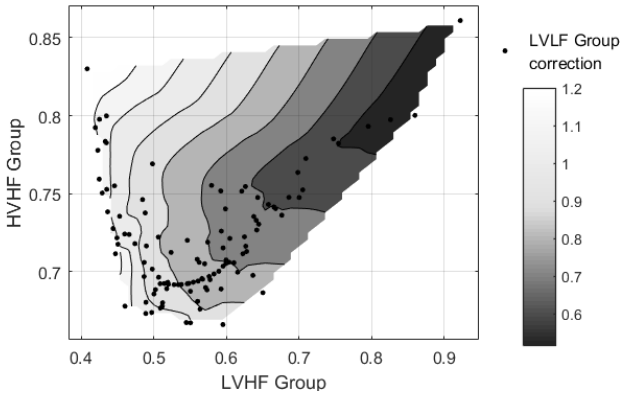

Figure 15 – Projection of Pareto surface on in LVHF-HVHF plot

front, and thus it is hard to reach an optimised correction for all the three objectives at the same time.

Table 3 shows the selected parameters of three points numbered in Figure 13 and 14, which are on different Pareto front but with different orientations. Table 4 shows one typical curve in each group for the three selected points in Table 3. With the parameters of point 1, the excitation of low frequency is well fitted and thus they are more applicable to the comfort test track. Point 2 and Point 3 are oriented to high frequency so they have worse corrections to low frequency comparing to Point 1.

	Point 1	Point 2	Point 3
A	0	0	0
B	-0.1	-0.1	-0.1
C	-150.5	-117	-146
α	85	265	179
δ	50	600	600
$log(\beta)$	4	4.33	5.6
$log(\gamma)$	2.65	2	4.26
n	5	7.5	8
μ	0	0.002	0
e_1	0.53	1.31	1.01
e_2	0.86	0.40	0.59
e_3	0.80	0.83	0.66

Table 3 – Resume of three points on Pareto Front

4.3 Post-treatment of Pareto front

Figure 16 shows the choice of α and n for the 15 best corrections to each group on Pareto front. Table 1 shows that the hysteresis force is relatively small for low frequencies, so the NSGA II proposed a smaller α comparing that to LVHF group. n has also a great impact on identification results and a smaller n is preferred for the LVLF group. It can be noticed that the interaction of parameters of Bouc-Wen model is not negligible which explains that several solutions with a smaller n also fit well with HVHF groups. These regimes can be served as reference data for the further robust analysis.

5 Comfort simulation

To validate the identified shock model, a comfort simulation in virtual proving ground has been realized. The full vehicle assembly has been posed on a virtual 4-cylinder test bench which provides 4 vertical degrees of freedom [16]. A simultaneous sweep frequency sinus signal (0.5Hz-6Hz) is defined as the displacement of 4

	Point 1	Point 2	Point 3
LVLF	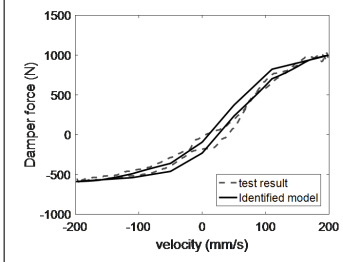	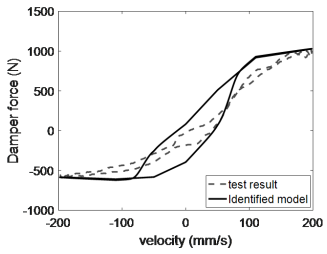	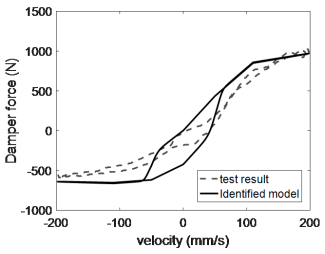
LVHF	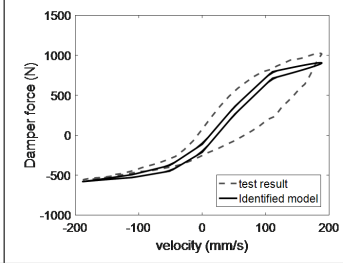	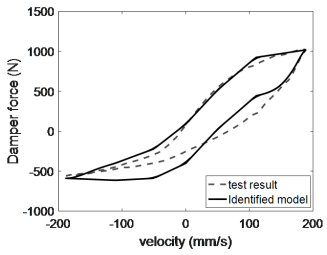	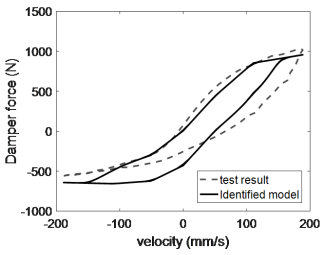
LVLF	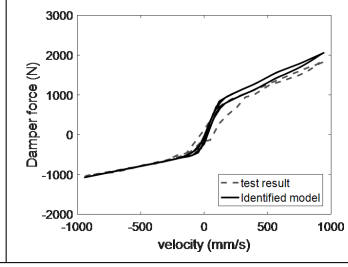	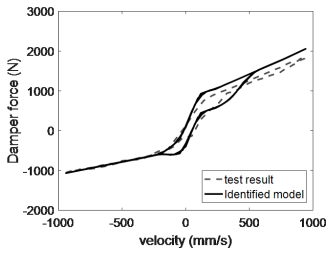	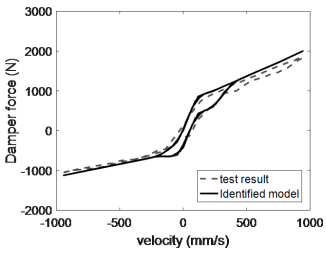

Table 4 – Correction of test results from choice of different orientations (Point 1: Best correction for low frequency. Point 2 and 3: Best corrections for high frequency)

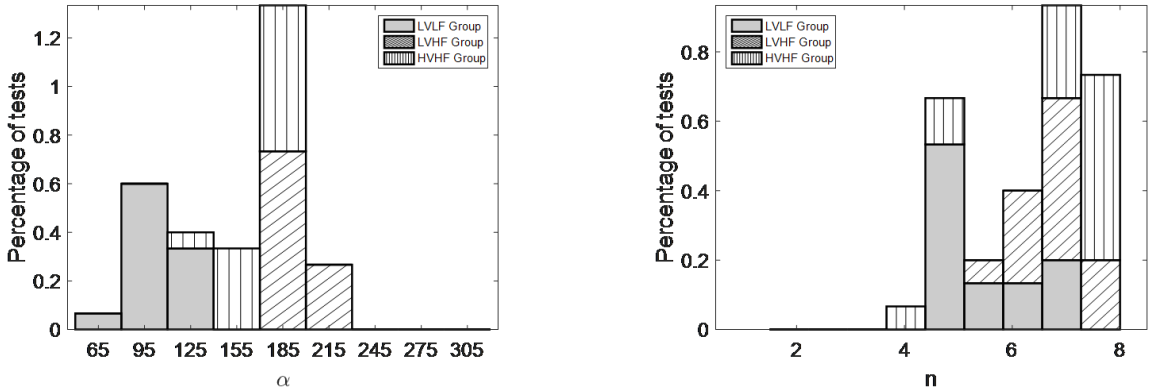

Figure 16 – Resumes of α (left) and n (right) of 15 best corrections in each group

cylinders (see Figure 17, 18).Two transfer functions of displacement from front or rear car body to the cylinder displacement have been calculated and serves as a criteria for ride comfort specification.

The best correction sets of low velocity regime and low frequency group of the modified Bouc-Wen model have been chosen for front and rear suspensions and are integrated into the full vehicle simulation. At the same time, the comparative simulations are launched with single curve models. The transfer function can be seen in Figure 19. With the modified Bouc Wen model, there is no great correction to the amplitude around the proper frequencies of front and rear suspensions. However, at the beginning phase of the signal, a richer model containing the hysteresis force can improve the quality of simulation especially for the rear suspension. The damper force at the first 20 seconds has shown that the shapes are very different for small excitations but after that the damper force from two models becomes almost identical.

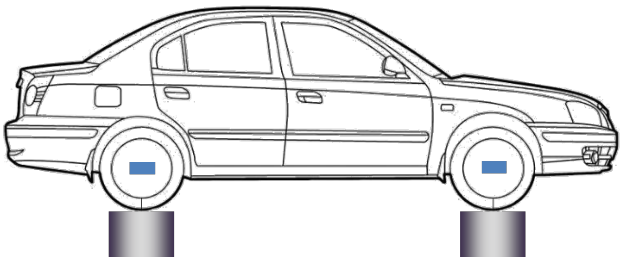

Figure 17 – The full vehicle comfort test bench

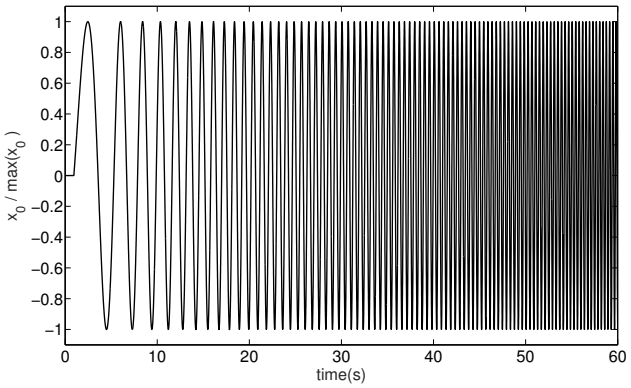

Figure 18 – One part of excitation signal

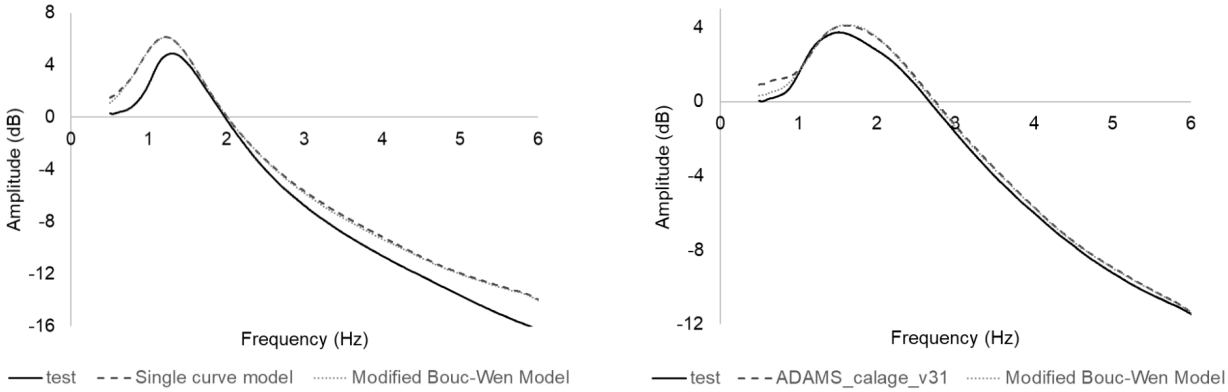

Figure 19 – Comparison of transfer function for front (left) and rear (right) suspensions

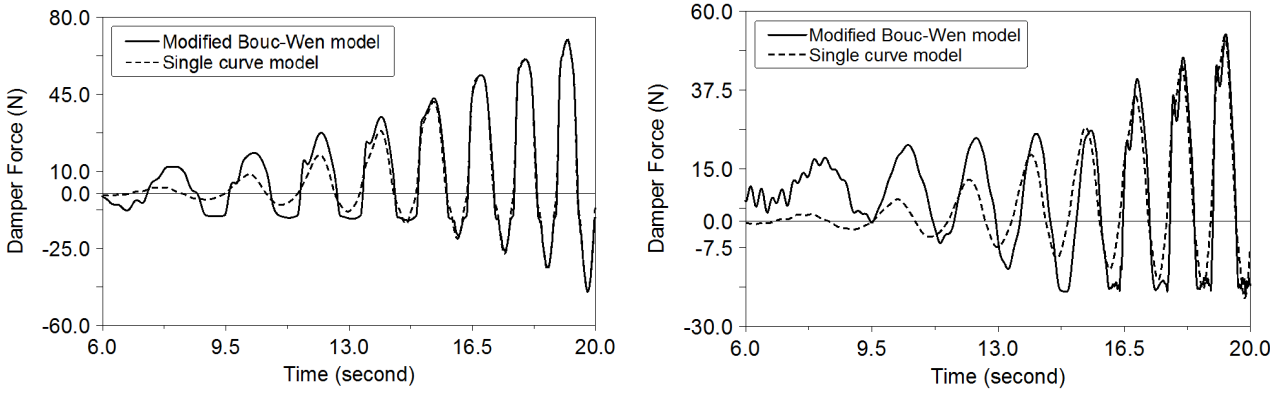

Figure 20 – Comparison of transfer function for front (left) and rear (right) suspensions

6 Conclusion and perceptive

In this article, a damper model based on Bouc-Wen model and its identification method are proposed. By a multi-objective optimization process, the model can reproduce the test curves with different velocities and frequencies. A comfort simulation in virtual ground orienting to low frequencies has been realized and it showed the impact of hysteresis model to the ride comfort prediction.

The next step will be the robust tests of parameters to the simulation results according to the analysis in Section 4.3 because measurements have shown that the curves may be slightly different for the two shock absorbers from the same technical definition.

References

References

[1] J. Arbiol, J. A. Muñoz, X. Armengo, and E. Aramburu, "Full vehicle durability analysis by means of the idiada virtual proving ground," in *Proceedings of the FISITA 2012 World Automotive Congress*. Springer, 2013, pp. 337–347.

[2] H. Wee, Y. Y. Kim, H. Jung, and G. N. Lee, "Nonlinear rate-dependent stick-slip phenomena: modeling and parameter estimation," *International Journal of Solids and Structures*, vol. 38, no. 8, pp. 1415–1431, 2001.

[3] G. Wang, G. Chen, and F. Bai, "Modeling and identification of asymmetric bouc–wen hysteresis for piezoelectric actuator via a novel differential evolution algorithm," *Sensors and Actuators A: Physical*, vol. 235, pp. 105–118, 2015.

[4] "A new method for damper characterization and real-time capable modeling for ride comfort."

[5] G. Yao, F. Yap, G. Chen, W. Li, and S. Yeo, "Mr damper and its application for semi-active control of vehicle suspension system," *Mechatronics*, vol. 12, no. 7, pp. 963–973, 2002.

[6] M. Sadeghi Reineh, "Physical modeling and simulation analysis of an advanced automotive racing shock absorber using the 1d simulation tool amesim," 2012.

[7] "Improved functional modelling in comfort analyses for hydraulic suspension testing."

[8] H.-B. Yun, S. F. Masri, R. W. Wolfe, and G. Benzoni, "Data-driven methodologies for change detection in large-scale nonlinear dampers with noisy measurements," *Journal of Sound and Vibration*, vol. 322, no. 1-2, pp. 336–357, 2009.

[9] B. Loyer, "Conception fonctionnelle robuste par optimisation multicritère de systèmes de suspension automobile passifs et semi-actifs," Ph.D. dissertation, Ecully, Ecole centrale de Lyon, 2009.

[10] M.-M. Chatillon, "Méthodologie de conception robuste appliquée aux trains de véhicules de tourisme," Ph.D. dissertation, Ecully, Ecole centrale de Lyon, 2005.

[11] P. R. Dahl, "A solid friction model," Aerospace Corp El Segundo Ca, Tech. Rep., 1968.

[12] A. Al Majid, "Dissipation de l'énergie en mécanique vibratoire: opérateur d'hystérésis, phénomène métrique," Ph.D. dissertation, Lyon, INSA, 2002.

[13] B. Spencer Jr, S. Dyke, M. Sain, and J. Carlson, "Phenomenological model for magnetorheological dampers," *Journal of engineering mechanics*, vol. 123, no. 3, pp. 230–238, 1997.

[14] N. Kwok, Q. Ha, M. Nguyen, J. Li, and B. Samali, "Bouc–wen model parameter identification for a mr fluid damper using computationally efficient ga," *ISA transactions*, vol. 46, no. 2, pp. 167–179, 2007.

[15] K. Deb, S. Agrawal, A. Pratap, and T. Meyarivan, "A fast elitist non-dominated sorting genetic algorithm for multi-objective optimization: Nsga-ii," in *International conference on parallel problem solving from nature*. Springer, 2000, pp. 849–858.

[16] P. G, "Déploiement et validation du confort," Renault, Rapport dâExpertise, 2018.